Research in Astronomy and Astrophysics, 24:095017 (9pp), 2024 September https://doi.org/10.1088/1674-4527/ad707a

Understanding the Impact of H_2 Diffusion Energy on the Formation Efficiency of H_2 on the Interstellar Dust Grain Surface

Xiaoying Guo[1], Wasim Iqbal[2,3], Qiang Chang[1], and Xiao-Hu Li[2,3]
[1] School of Physics and Optoeletronic Engineering, Shandong University of Technology, Zibo 255000, China
[2] Xinjiang Astronomical Observatory, Chinese Academy of Sciences, Urumqi 830011, China; wasim@xao.ac.cn
[3] Key Laboratory of Radio Astronomy, Chinese Academy of Sciences, Urumqi 830011, China
Received 2024 June 22; revised 2024 August 6; accepted 2024 August 8; published 2024 September 18

Abstract

We use microscopic Monte Carlo simulation techniques to investigate the impact of H_2 diffusion energy on the recombination efficiency of H_2 on interstellar dust grain surfaces under diffuse and translucent cloud conditions. We constructed five models representing different possible conditions encountered by adsorbed H and H_2 on interstellar dust grains. We implemented adsorption sites with multiple binding energies for surface species; the Encounter-Desorption mechanism was also included. The study focused on silicate surfaces in diffuse clouds and water ice surfaces in translucent clouds. The results show that the recombination efficiency of H_2 on dust surfaces decreases as H_2 diffusion energy increases. An interesting finding of this work is that considering different binding sites for H and H_2 gives rise to multiple steady phases, during which the recombination efficiency remains constant with a change in H_2 diffusion energy.

Key words: astrochemistry – atomic processes – ISM: molecules

1. Introduction

Molecular hydrogen (H_2) is the most abundant molecule in the universe. Almost all the hydrogen is in its molecular form in the dense and translucent clouds. Because of its abundance, H_2 plays a critical role in much of the chemistry in the star-forming regions (Cazaux & Tielens 2002, 2004; Wakelam et al. 2017; Bialy & Sternberg 2019; Tacconi et al. 2020; Chevance et al. 2022; Nakazato et al. 2022). H_2 is also overwhelming present in various other regions of the interstellar medium (ISM) such as photon-dominated regions, outflows of planetary nebulae, jets, shocks, and supernova remnants (Cazaux & Tielens 2004; Iqbal et al. 2012). Ion-molecule reactions involving H_2 and dissociative recombination processes are crucial steps in the chemical pathways leading to numerous simple and abundant interstellar species (Cazaux & Tielens 2002, 2004; Wakelam et al. 2017). Additionally, H_2 is the primary collider in dense clouds and serves as an important coolant, particularly in regions of warm gas (Herbst & Klemperer 1973; Cazaux & Tielens 2004; Sternberg 2006; Bialy & Sternberg 2015). Since H_2 plays a key role in determining the physical and chemical evolution of the ISM, the study of how H_2 is formed remains of fundamental importance.

Studies in the past few decades have established that the gas-phase formation rate of H_2 in the ISM is inefficient in explaining the observed abundance of molecular hydrogen, and one needs to focus on different formation mechanisms on interstellar dust grains to produce the observed abundance of H_2 (Gould & Salpeter 1963; Herbst & Klemperer 1973; Cazaux & Tielens 2002, 2004; Iqbal et al. 2014; Wakelam et al. 2017). However, the exact mechanism of H_2 formation on dust grain surfaces remains a subject of intense focus.

In the literature, we find that researchers have mostly concentrated on the Langmuir–Hinshelwood (LH) mechanism at low temperatures to study H_2 formation on dust surface (Watson & Salpeter 1972; Tielens & Allamandola 1987; Cazaux & Tielens 2004; Iqbal et al. 2012; Wakelam et al. 2017). In this mechanism, H atoms accrete on dust grains and then adsorb onto the dust surface through a process known as physisorption, facilitated by weaker binding energies. Once adsorbed, the H atoms overcome the diffusion energy and hop across the dust surface. When an H atom encounters another H atom while hopping, a chemical reaction occurs, forming a H_2 molecule. Additionally, H atoms can also desorb from the dust surface if they get energy higher than the desorption energy. The desorption and diffusion rates of an H atom increase rapidly with the surface temperature (T) as it is governed by the equation $\exp(-\frac{E}{T})$, where E is the diffusion or desorption energy in K. To account for efficient H_2 formation, an H atom must remain on the surface long enough to meet another H atom and form H_2. To facilitate this, (1) the surface temperature must be such that the desorption probability is significantly lower than the encounter probability of two H atoms on the surface, and (2) the temperature should be high enough to enable efficient hopping of H atoms. These requirements ask for conflicting conditions that are hard to meet in various astronomical sources in the ISM. Recent research shows that a possible solution to this conflict could be in the treatment of the

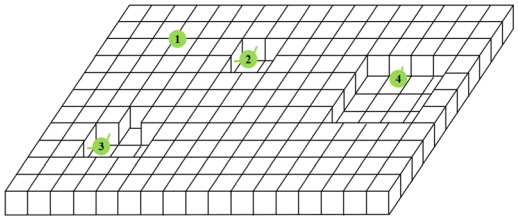

Figure 1. A schematic of lateral bonds formed by species at different binding sites and the neighboring positions on dust grain surface. (The green ball is the adsorbed species.)

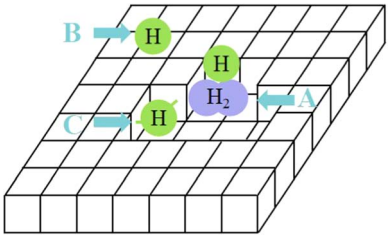

Figure 2. A schematic representation when an H atom accretes to a binding site already occupied by H_2. (The green one is the adsorbed H, and the blue one is the adsorbed H_2.)

desorption energy of H atoms, which is not as uniform as previously assumed in chemical models but follows a Gaussian distribution (Grassi et al. 2020).

Further, since H atoms do not react with H_2 on grain surface, early models did not consider the presence of H_2 on the dust surface. However, Hincelin et al. (2015) introduced the Encounter-Desorption (ED) mechanism, demonstrating that adsorbed H_2 on dust surfaces can affect the formation of H_2. Chang et al. (2021) extended the ED mechanism to include both H and H_2. Zhao et al. (2022) used ED mechanism in their simulations and confirmed that the presence of adsorbed H_2 on dust surface affects the recombination efficiency of H_2. Their findings indicated that the diffusion energy of H_2 on the dust surface could impact the recombination efficiency of H_2. However, Zhao et al. (2022) did not investigate how uncertainties or variations in the diffusion energy of H_2 on grain surface impacts the recombination efficiency of H_2, and also, in the literature we do not find any work done previously to investigate it. Hence, this study further improves on the work presented in Zhao et al. (2022) by investigating various models to understand the impact of diffusion energy of H_2 on the recombination efficiency of surface H_2.

This paper is structured as follows: Section 2 introduces the model developed. Section 3 explains the numerical methods used. The results of the numerical simulations are presented in Section 4. Finally, Section 5 provides a summary and discussion.

2. Model Description

Following the work of Zhao et al. (2022), we consider three types of binding sites on the grain surface, namely the shallow binding sites, the medium binding sites, and the deep binding sites. The reason for choosing only three types of binding sites is already explained in detail in Zhao et al. (2022), so we do not discuss it here in further detail. The binding energy at the medium binding sites is 40% higher than that at the shallow binding sites and 40% lower than that at the deep binding sites (again, see Zhao et al. 2022 for details).

In Figures 1 and 2, we illustrate the possible scenarios on the dust grain surface implemented in our model in this work. Initially, during the accretion process, the sites on the dust grain surfaces are unoccupied by other species, and each site can accommodate up to four layers of species on top of each other (generally not more than two layers are formed in our simulations, so to be on the safe side we implemented a 4-layer model). Only the species on the first layer are connected with the grain surface. Species on the higher layers do not interact with the surface. When an atom or a molecule from the gas phase accretes to a site without any horizontal neighbors, it forms a vertical bond with the dust grain surface (species 1 in Figure 1), indicating a shallow binding site. If the accretion site of the species already has one horizontal neighbor, then the species forms both a vertical bond with the surface and a lateral bond with the horizontal neighbor (species 4 in Figure 1), indicating a medium binding site. When the accretion site has two horizontal neighbors, then the species forms two lateral bonds in addition to the vertical bond (species 2 and 3 in Figure 1), indicating a deep binding site.

However, when an atom or a molecule accretes to a site on the dust grain surface that is already occupied by another atom or molecule, the aforementioned situation changes. This is explained using H and H_2 as an example in Figure 2. As shown in Figure 2, when an H atom accretes to site A, which is already occupied by an H_2, it cannot form lateral bonds with the two horizontal neighbors available at site A. Consequently, deep binding site A, with a significantly higher effective binding and diffusion energy (similar to site C), behaves as a shallow binding site (similar to site B with no lateral binding sites) due to the presence of an adsorbed H_2 molecule. Similarly, a medium or deep binding site behaves as a shallow binding site when occupied by an H atom. This is called the ED mechanism, as mentioned earlier.

Other parameters to consider here are the binding and diffusion energies on different substrate. For example, on an H_2 substrate, the desorption energies for H_2 and H are significantly lower than those on silicate and water ice. Calculations indicate that at a temperature of 10 K, the desorption energy of H on an H_2 substrate ($E_{D,\mathrm{H-H_2}}$) is 45 K, while the desorption energy of H_2 on an H_2 substrate ($E_{D,\mathrm{H_2-H_2}}$) is approximately 23 K (Pierre et al. 1985; Vidali et al. 1991). Recent quantum chemical calculations by Das et al. (2021) found that $E_{D,\mathrm{H_2-H_2}}$ varies between 67 and 79 K, and $E_{D,\mathrm{H-H_2}}$ varies between 23 and 25 K.

Table 1
Summary of Models

Model	Astronomical Sources	R	$R_{H_2} = R_H$	E_{D,H_2-H} (K)	E_{D,H_2-H_2} (K)	$E_{D,H-H_2}$ (K)	μ	If Binding Sites for H and H_2 are same
M01	diffuse clouds	0.8	0.8	30	23	45	1	yes
M02	diffuse clouds	0.8	0.8	30	23	45	0	yes
M03	diffuse clouds	0.8	0.8	30	73	24	1	yes
M04	diffuse clouds	0.8	0.8	30	23	45	1	no
M05	translucent clouds	0.44	0.44	30	23	45	1	yes

Further, H atoms also have the ability to enhance the desorption rate of H_2. According to estimates presented in Cuppen & Herbst (2007), $E_{D,H_2-H} = 30$ K, which is significantly lower than the desorption energy of H_2 on bare silicate surface. To account for this, in our model the desorption energy of H_2 is reduced to 30 K whenever a H_2 molecule occupies a site previously held by an H atom. This emphasizes the role of H in regulating the desorption rate of H_2. Therefore, in our model, the diffusion and desorption energies for H_2 on different surface such as top of an H atom, H_2 molecule, and bare dust grain surface are considered to be different. Similarly, the diffusion and desorption energies for H on top of H_2 substrate and bare dust grains are different.

In this work, our aim is to investigate the H_2 formation efficiency on the interstellar dust surfaces in the diffuse and translucent clouds, taking into account the possible variations in H_2 binding and diffusion energies on different types of surfaces. According to Biham et al. (2001), the gas phase temperature in diffuse clouds is around 100 K, with dust grains consisting of silicate surfaces. Meanwhile, according to Wakelam et al. (2017), the gas phase temperature in translucent clouds ranges from 15 to 40 K, with dust grains covered by water ice surfaces. To account for these differences in different types of sources, we construct four models (M01, M02, M03, and M04) to investigate the effect of the diffusion energy of H_2 on the formation efficiency of H_2 on the silicate surface. Additionally, a fifth model, M05, was developed to study the effect of the diffusion energy of H_2 on water ice on the formation efficiency of H_2. In our models, we also use a parameter μ to represent what percentage of newly formed H_2 is instantly released in the gas phase through a process called chemical desorption (Garrod et al. 2007).

In model M01, the desorption energies of H_2 and H on the H_2 substrate are 23 K and 45 K, respectively and the chemical desorption coefficient μ is set to "1" which means all newly formed H_2 is released instantly in the gas phase. To investigate the effect of μ on H_2 formation efficiency, model M02 was run with the value of μ set to "0" while all other parameters are kept the same as in model M01.

To the best of our knowledge, the specific values of E_{D,H_2-H} and E_{D,H_2-H_2} are not well described in the literature. We could only find that Pierre et al. (1985), Vidali et al. (1991), and Das et al. (2021) provide different values as discussed earlier. Hence, to test the impact of a different possible values for E_{D,H_2-H} and E_{D,H_2-H_2} on H_2 formation efficiency, we run model M03. This model is similar to M01, but with E_{D,H_2-H_2} and $E_{D,H-H_2}$ set to 73 K and 24 K, respectively. In models M01, M02, and M03, we assume that the deep binding sites for H atoms are also deep binding sites for H_2 molecules, which is a general case. To test a more specific case where deep binding sites are different for different species, we run model M04, in which the deep binding sites for H atoms and H_2 molecules are not the same. In models, M01-M04, H_2 diffusion energy on dust grain surfaces was varied from 308 to 488 K in increments of 12 K to study the effect of the diffusion energy on the recombination efficiency of H_2 on dust grain surfaces. Finally, the parameter R in the model is the ratio of diffusion energy to desorption energy on an empty binding site. The ratio between the diffusion energy and desorption energy of a surface species on sites occupied by H_2 is R_{H_2} and the ratio of H_2 diffusion energy to its desorption energy on sites occupied by H atoms is R_H. Table 1 lists parameters described above in different models.

Model M05 was designed to investigate the effect of the diffusion energy of H_2 on the synthesis of H_2 on dust grain surfaces in translucent clouds, where the dust grain surface is assumed to be covered with water ice. In this model, the diffusion energies of H and H_2 at sites occupied by H_2 are 45 K and 23 K, respectively. The diffusion energy of H_2 on water ice was varied, increasing from 194 to 356 K in steps of 9 K.

In Table 2, we summarize the diffusion and desorption energies at shallow, medium, and deep binding sites on dust surfaces that are not occupied by H_2. Following the work of Wakelam et al. (2017), the desorption energies (for medium binding sites) used for H atoms on silicate surface and water ice are 510 K, and 580 K, respectively.

3. Numerical Method

This study employed the Microscopic Monte Carlo (MMC) method for simulations. For MMC simulations, binding sites on interstellar dust were arranged in a square lattice with total number of sites $(N_s) = L^2$, where L represents the square root of the total number of sites on the dust surface. Tiné et al. (1997) suggested that setting L to 100 was sufficiently large to eliminate finite-size effects. Therefore, L was fixed at 100 in

Table 2
Desorption and Diffusion Energies of H and H_2 on the Silicate Surface and Water Ice

	H_2 on Silica (M01-M04)	H_2 on Water Ice (M05)	H on Siliates (M01-M04)	H on Water Ice (M05)
Desorption energy (K)	varies with model	varies with model	(306, 510, 715)	(348, 580, 812)
Diffusion energy (K)	varies with model	varies with model	(244, 406, 568)	(153, 255, 357)

Note. In (a, b, c): a, b, and c are energies for the shallow, medium, and deep binding sites, respectively.

this study, which saved significant computational time. Each site on the square lattice has four nearest neighboring sites. Species from the gas phase can adsorb onto these sites, becoming surface material on the lattice. These species can randomly hop from one site to any of their nearest neighboring sites. We keep tracking the position of each surface species during the process. When two reactants are located at the same site, a chemical reaction occurs. In our models, the only possible reaction that can occur is between H atoms to form H_2. Whether H_2 remains on the dust surface depends on the value of μ as described earlier. An adsorbed species can also desorb from the surface if it has energy larger than desorption energy.

In our model, H_2 is formed immediately on recombination of two H atoms. So, there is no separate time calculated for H recombination event. Thus, there are only three types of events in our simulation: accretion, hopping, and desorption. We calculate the absolute time for each event (accretion, hopping, and desorption) to occur. The event corresponding to the smallest time is found and executed. The system time is reset to this time. We check it again which is the next event in the list of events and execute it and increase the system time to the execution time of that event. Thus, the system time evolves with each execution of events until a fixed time is reached and simulation is terminated.

The accretion rate of a species depends on its accretion flux, which is a function of gas temperature and the density of the species and can be written for H as follows,

$$f_{\rm H} = \frac{v_{\rm H} n_{\rm H}}{4 n_s}, \tag{1}$$

where $v_{\rm H}$ and $n_{\rm H}$ are, respectively, average velocity and number density of H in the gas phase, and n_s is number density of sites on the grain surface. The expression for $v_{\rm H}$ is,

$$v_{\rm H} = \sqrt{\frac{8 k_{\rm B} T_{\rm gas}}{\pi m_{\rm H}}}, \tag{2}$$

where $m_{\rm H}$ is mass of H atom, $T_{\rm gas}$ is the gas temperature, and $k_{\rm B}$ is Boltzmann's constant. The accretion rate R_{AH} of H atoms in the units of atoms per sec is given by,

$$R_{AH} = 4\sigma n_s f_{\rm H}, \tag{3}$$

where σ is the cross section of the dust grain which is assumed to be spherical. Now, total number of binding sites on grain surface is given as,

$$N_s = 4\sigma n_s. \tag{4}$$

Using Equations (3) and (4), we obtain,

$$R_{AH} = N_s f_{\rm H}. \tag{5}$$

Similarly for H_2, we can write,

$$R_{AH_2} = N_s f_{\rm H_2}. \tag{6}$$

In our model, we assume an H density ($n_{\rm H}$) of 10 $\rm cm^{-3}$ for the diffuse cloud and a gas temperature of 100 K (Biham et al. 2001). Thus, accretion flux of atomic hydrogen in the diffuse cloud (using Equation (1)) is $f_{\rm H} = 1.8 \times 10^{-9}$ ML $\rm s^{-1}$, and we considered that 50% of hydrogen nuclei in the diffuse cloud have already converted to H_2. Thus, effective $f_{\rm H}$ becomes 9×10^{-10} ML $\rm s^{-1}$. We recall that $N_s = L^2 = 10^4$. Thus we get $R_{AH} = N_s f_{\rm H} = 9 \times 10^{-6}$. Similarly, the accretion rate of H_2 is calculated to be 3.18×10^{-6} ML $\rm s^{-1}$.

In translucent clouds, we assume a gas temperature of 30 K and a hydrogen nucleus density of 1000 $\rm cm^{-3}$ (Wakelam et al. 2017). Under translucent cloud conditions, we assume that 75% of the hydrogen nuclei have already converted to H_2, resulting in an H flux of 1.3×10^{-8} ML $\rm s^{-1}$. Using this in Equation (5), we get the accretion rate of H to be 3.275×10^{-5} ML $\rm s^{-1}$. Similarly, the accretion rate of H_2 is 3.474×10^{-5} ML $\rm s^{-1}$.

After accretion, species on the dust grain surface can either hop to one of the neighbor sites or desorb to the gas phase. The accretion and desorption rates are calculated, respectively, using the following equations,

$$b_1 = \nu \exp\left(-\frac{E_b}{T}\right), \tag{7}$$

$$b_2 = \nu \exp\left(-\frac{E_D}{T}\right), \tag{8}$$

where ν is called the attempt rate, and is set at 10^{12} $\rm s^{-1}$. E_b and E_D are the diffusion and desorption energies of the species on the dust grain surface, and T is the temperature of the dust grain surface. We calculate b_1 and b_2 for both H and H_2 using respective values of parameters.

Both hopping and desorption are random processes and there is race between hopping and desorption. To know if the species will hop or desorb, we use a random number X between [0, 1]

and compare called value of X with the following expression,

$$X < \frac{b_1}{b_1 + b_2}. \quad (9)$$

If Equation (9) is true then the species hops, otherwise, it is desorbed to the gas phase.

In our simulations, the waiting time for the accretion of H is obtained using the following equation,

$$\tau_1 = -\frac{\ln(Y)}{R_{AH}}, \quad (10)$$

where Y is another random number, also between [0, 1], and R_{AH} is the accretion rate of H obtained using the Equation (5). Similarly, we also calculate the accretion time (τ_2) for H_2.

Again, the times for hopping or desorption for both H and H_2 are calculated using the following equation,

$$\tau_3 = -\frac{\ln(Y)}{b_1 + b_2}, \quad (11)$$

where b_1 and b_2 are calculated using Equations (7) and (8).

At the beginning of the simulation, the surface population of H and H_2 fluctuates but keeps increasing with simulation time. Over time, the population of H and H_2 reaches a steady state and starts to fluctuate around a constant value. Once the steady state is achieved, a sufficiently large time interval τ' is selected. Simulation is allowed to run in the steady state for this time interval τ' and then terminated. The time τ' is chosen to be sufficiently large to ensure that there is a minimum statistical error in the calculation of H_2 formation efficiency η due to the fluctuation in H and H_2 surface population during the steady state. At the end of time τ', we calculate the total number of H_2 formed (N_{H_2}) and the total number of H adsorbed (N_H) during the time τ'. Finally, the recombination efficiency η is determined using the following equation,

$$\eta = \frac{2N_{H_2}}{N_H}. \quad (12)$$

4. Research Results

In this section, we present our results for different models (M01-M05), divided into two sections: diffuse clouds and translucent clouds.

4.1. Diffuse Clouds

In this subsection, we present results for diffuse cloud conditions using representative models M01-M04. Panel (A) in Figure 3 shows the effect of H_2 diffusion energy on H_2 recombination efficiency η on dust grain surface with the surface temperatures of 10, 12, and 15 K and using model M01. Here we note that, for any given surface temperature, the recombination efficiency η decreases with increasing H_2 diffusion energy. To better understand the simulation outcome, the total numbers of H and H_2 occupying shallow, medium, and deep binding sites in steady state are plotted, respectively, in panels (A) and (B) in Figure 4, all results are for simulation with 10 K surface temperature. We note that, as the diffusion energy of H_2 increases, more and more H_2 are likely to occupy deep binding sites, and when the diffusion energy of H_2 reaches approximately 375 K, almost all deep binding sites are occupied by H_2. Since in model M01 presented here, the deep binding sites for H_2 are also the deep binding sites for H, the presence of H_2 in all the deep sites causes fast desorption of surface H atoms due to the ED mechanism explained earlier. Consequently, H atoms do not stay long enough on the grain surface to make H_2, resulting in a sharp decrease in the recombination efficiency with increasing H_2 diffusion energy.

Panels (B), and (C) in Figure 3 show the recombination efficiency η as a function of H_2 diffusion energy on the dust surface (at different surface temperatures of 10 K, 12 K, and 15 K) in models M02, and M03, respectively. These results are similar to results obtained in model M01 and shown in Panel (A) in Figure 3. This indicates that the instant desorption of newly formed H_2 and the diffusion energies of H and H_2 on the H_2 substrate have negligible impact on the recombination efficiency of H_2 on the dust surface. Therefore, these cases are not discussed in more detail in this work.

We present our simulated H_2 recombination efficiency as a function of H_2 diffusion energy for model M04 in Panel (D) in Figure 3, where black, red, and blue lines represent the cases for different surface temperatures of 10 K, 12 K, and 15 K, respectively. The only difference in model M04 compared to model M01 is that the deep binding sites for H atoms and H_2 are different in model M04. Similar to model M01 results, the results obtained here also show that, at a fixed surface temperature, the H_2 recombination efficiency decreases with increasing H_2 diffusion energy. However, unlike model M01, we find in model M04 that there are multiple steady phases between certain ranges of H_2 diffusion energy. Within this range of H_2 diffusion energy, H_2 recombination efficiency remains constant. For example, at a surface temperature of 12 K, H_2 recombination efficiency remains constant when H_2 diffusion energy changes from 308 to 368 K and again from 428 to 488 K.

To explain this dependence of H_2 recombination efficiency on H_2 diffusion energy, we plotted the statistical distribution of H atoms (Figure 4, panel (C)) and H_2 (Figure 4, panel (D)) at shallow, medium, and deep binding sites at 10 K surface temperature. Here in the panel (D) in Figure 4, we can see that with increasing H_2 diffusion energy, more and more H_2 diffuse to deep binding sites, causing an increase in H_2 population on grain surface, and hence H population decreases due to the stronger impact of the ED mechanism. This trend continues until H_2 diffusion energy has reached approximately 375 K, and at this point, all deep binding sites are filled with H_2 causing the impact of the ED mechanism (arising due to H_2

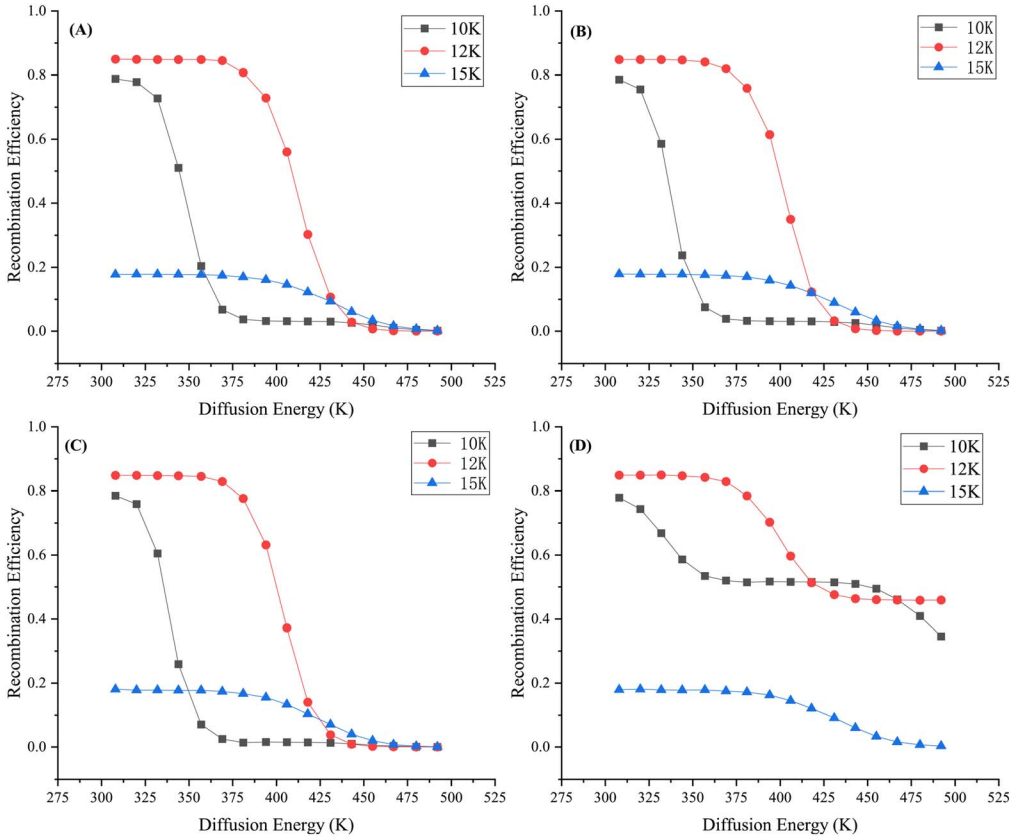

Figure 3. Panels (A), (B), (C), and (D), respectively, show the simulated relation between the H_2 recombination efficiency η and H_2 diffusion energy on the dust grain surface with different surface temperatures as calculated using model M01, M02, M03, M04.

sitting in deep binding sites) to reach its maximum. Hence, we see no further change in H population on the grain surface, and H_2 recombination efficiency becomes constant and remains so until H_2 diffusion energy is approximately 425 K. Once H_2 diffusion energy is further increased, we notice a transition as more and more H_2 now start to occupy medium binding sites (see the rising red curve in the panel (D) in Figure 4). Now, the H_2 population on the grain surface starts to increase with increasing H_2 diffusion energy, causing a stronger impact of the ED mechanism on the H atom population on the grain surface. As a result, the H atom population on the grain surface starts to decrease again, causing a gradual decrease in H_2 recombination efficiency.

4.2. Translucent Clouds

In this subsection, we discuss results for translucent cloud conditions (Zhao et al. 2022) using representative model M05.

In Figure 5, we show the effect of H_2 diffusion energy on the recombination efficiency on dust surfaces at temperatures of 12 K (black lines), and 15 K (red lines) using the model M05. According to Zhao et al. (2022), 12 and 15 K are the critical temperatures under translucent cloud conditions, where changes in the recombination efficiency on water ice occur. Therefore, these two temperatures were chosen for the study. In Figure 5, it can be seen that (at the same surface temperature) the recombination efficiency of H_2 on the dust surfaces decreases as the diffusion energy of H_2 on dust surfaces continuously increases, highlighting the impact of H_2 diffusion energy on water substrate in translucent clouds-like conditions.

5. Discussion

In this work, we use five different models (M01-M05) to do a detailed study to understand how the desorption energy of H_2 on the bare dust grain surface (silicate) with three different types of binding sites and the dust grain surface with a water substrate affects the recombination efficiency of H_2. The major finding of this research is that (on both silicate surface and water ice) the recombination efficiency of H_2 on dust grain surfaces decreases as the desorption energy of H_2 increases.

Results obtained from models M01-M03 show that the instant desorption of newly formed H_2 and the desorption energy of H and H_2 on H_2 substrate have negligible impact on the recombination efficiency of H_2 on the dust grain surfaces.

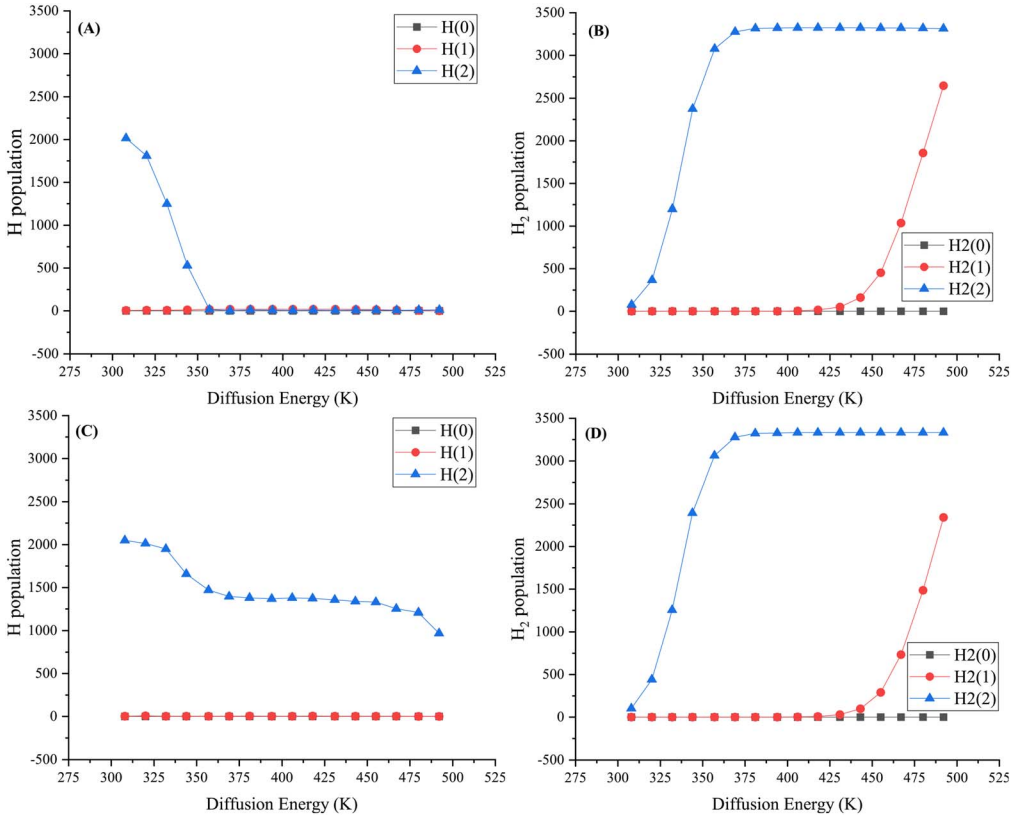

Figure 4. Panel (A): The number of hydrogen atoms occupying different binding sites. Here, H(0), H(1), and H(2) are, respectively, the number of hydrogen atoms in the shallow, medium, and deep binding sites. Panel (B): The number of H_2 occupying different binding sites. Here, H2(0), H2(1), and H2(2) are, respectively, the number of H_2 in the shallow, medium, and deep binding sites. Both (A) and (B) panels are for model M01 at 10 K surface temperature. Panels (C) and (D) are same as panels (A) and (B), respectively, but for model M04.

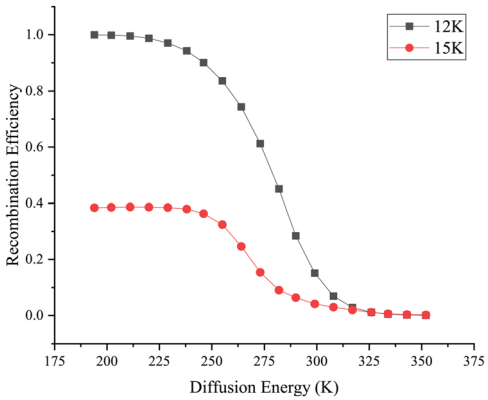

Figure 5. The relation between the recombination efficiency η and the diffusion energy of H_2 on the dust surface as calculated in the model M05.

We also find (comparing model results from M01 and M04) that H_2 recombination efficiency is higher when the deep binding sites for H are not the same as those for H_2. Under such conditions, a higher population of H_2 does not limit deep potential well available to H, even if H_2 occupies all the deep binding sites available to H_2, there are still separate deep binding sites available for H atoms to adsorb. As a result, the surface can retain H atoms in deep binding sites specific to H atoms. These H atoms help to produce H_2 efficiently.

Although our model results show that the H_2 diffusion energy is important for the recombination efficiency, this energy value is not well known yet. Recently, Meng et al. (2023) found that the ratio of H_2 diffusion energy to its desorption energy is approximately 0.57 on diamond-like carbon (DLC) surfaces based on the experimentally measured coverage dependent desorption energy of H_2 on DLC surfaces (Tsuge et al. 2019). Assuming this ratio on the DLC surfaces is the same as that on the silicate surfaces, the diffusion energy of H_2 is about 350 K in the medium binding sites on silicate surfaces. If the diffusion energy of H_2 is 350 K, Models M01 and M02 predict that the recombination efficiency is approximately 0.3, 0.85, and 0.2 at 10 K, 12 K, and 15 K respectively. On the other hand, Gry et al. (2002) found that the minimum H_2 recombination efficiency is 0.5 based on the observed H_2 formation rate in the diffuse ISM. Therefore, models M01 and M02 still underestimate the recombination efficiency at 10 and 15 K. Similarly, model M03 also underestimates the recombination efficiency at 10 and 15 K while model M04 can reasonably well estimate the

recombination efficiency at 10 and 12 K if the diffusion energy of H_2 is 350 K.

An interesting finding of this work is that considering different binding sites for H and H_2 gives rise to multiple steady phases, during which the recombination efficiency remains constant with a change in H_2 diffusion energy. The first steady phase starts when all deep binding sites are filled with H_2 and the second steady state starts when all medium binding sites are filled with H_2.

The proposed model only considered physisorption, although H can also chemisorb onto silicate or carbon surfaces. It remains unclear if considering both chemical adsorption and encounter desorption mechanisms in future work will help to better explain the formation efficiency of H_2 in diffuse clouds. Further research is necessary to uncover the mysteries of H_2 formation in diffuse clouds.

Acknowledgments

This work was supported by the National Natural Science Foundation of China (No. 12173023). W. I. thanks the Xinjiang Tianchi Talent Program (2024). We thank our anonymous referee who provided us with the valuable and constructive comments to improve the quality of the manuscript.

Appendix A
Extra Figures Showing the Relationship between the Difference in Diffusion Barriers between Mid and Deep Binding Sites, and the Ratio of H_2 Population at Mid and Deep Binding Sites

The plots in Figure A1 show the relationship between the H_2 population (in the mid and deep binding sites) and the energy difference between the mid and deep binding sites. The left and right panels, in Figure A1, are for models M01, and M04, respectively. From the plots, it can be observed that they do not simply follow a Boltzmann distribution. This complexity arises because our simulations incorporate encounter desorption mechanisms, which complicate the situation when species on the dust surface react. This affects the distribution observed. When the dust grain temperatures are 12 K or 15 K, the H_2 content on the dust surface is relatively low, hence closer to a Boltzmann distribution. However, at 10 K, where the H_2 content on the dust grain surface is higher, the impact of the encounter desorption mechanism is significant, leading to a distribution that differs significantly from that observed at 12 K or 15 K.

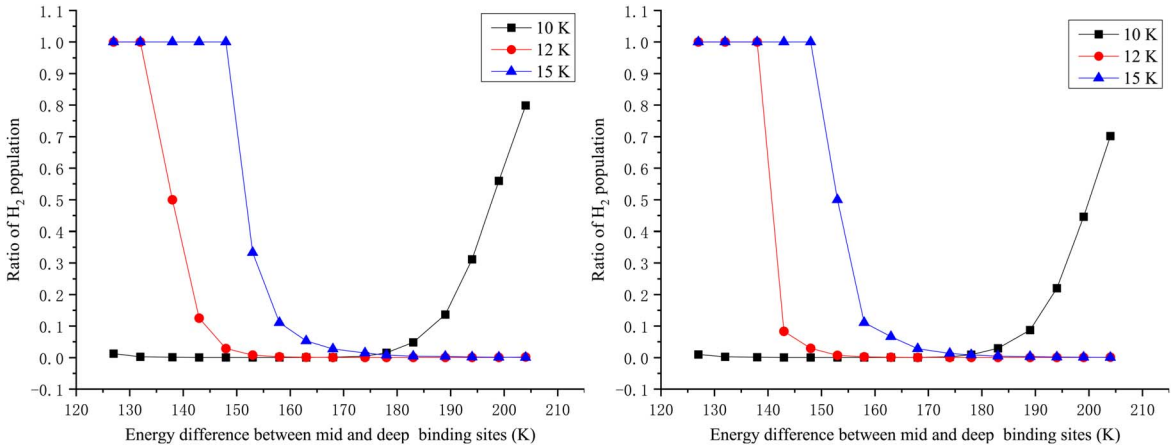

Figure A1. Plot showing the relationship between the H_2 population (in the mid and deep binding sites) and the energy difference between the H_2 population in the mid and deep binding site as a function of energy difference between the mid and deep binding sites. The left and right panels are for models M01, and M04, respectively.

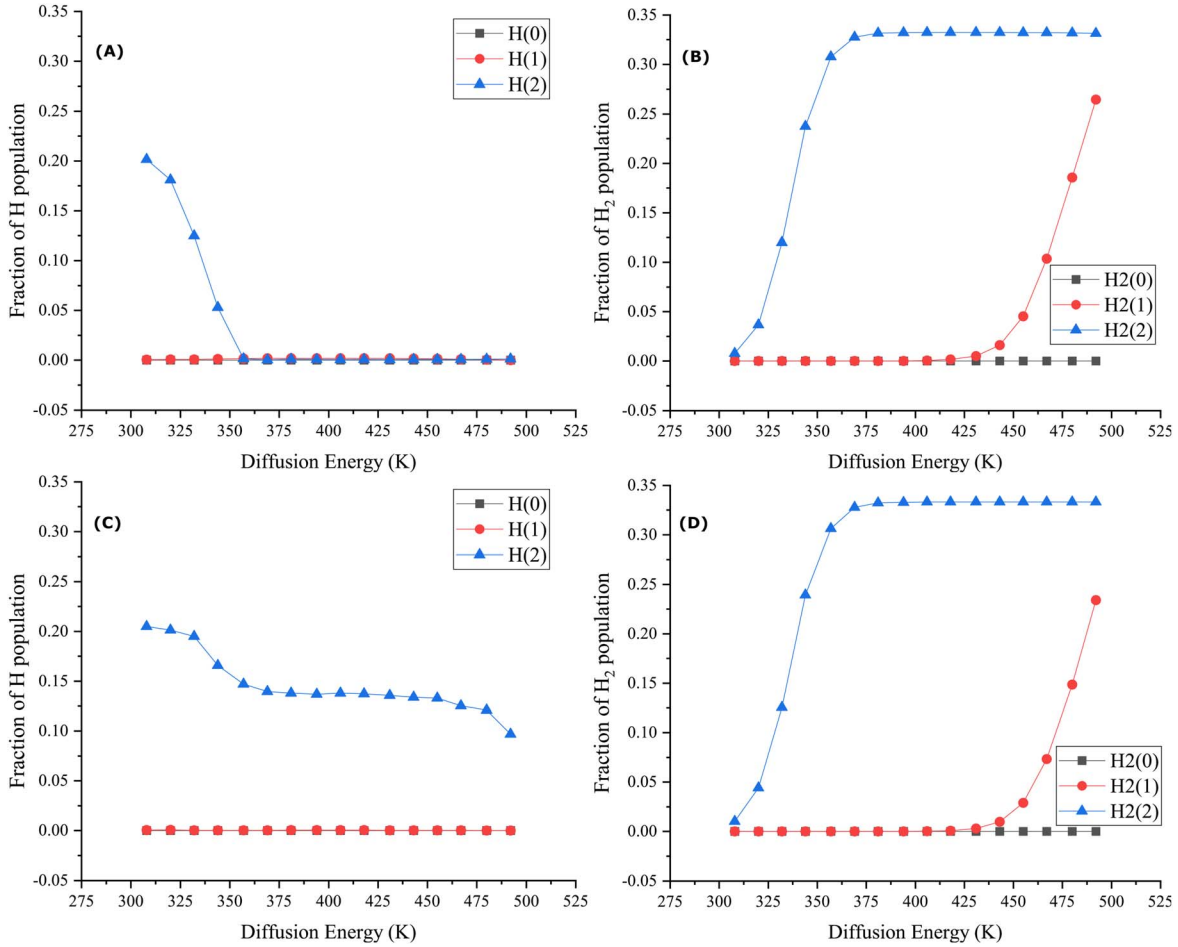

Figure B1. Panel (A): The fraction of hydrogen atoms occupying different binding sites. Here, H(0), H(1), and H(2) are, respectively, the fraction of hydrogen atoms in the shallow, medium, and deep binding sites. Panel (B): The fraction of H_2 occupying different binding sites. Here, H2(0), H2(1), and H2(2) are, respectively, the fraction of H_2 in the shallow, medium, and deep binding sites. Both (A) and (B) panels are for model M01 at 10 K surface temperature. Panels (C) and (D) are same as panels (A) and (B), respectively, but for model M04.

Appendix B
Extra Figures for Fractional H and H_2 Population on Grain Surface as a Function of H_2 Diffusion Energy

The Plots in Figure B1 are same as Figure 4, but show fraction of H and H_2 population instead of actual surface population.

References

Bialy, S., & Sternberg, A. 2015, MNRAS, 450, 4424
Bialy, S., & Sternberg, A. 2019, ApJ, 881, 160
Biham, O., Furman, I., Pirronello, V., & Vidali, G. 2001, ApJ, 553, 595
Cazaux, S., & Tielens, A. G. G. M. 2002, ApJL, 575, L29
Cazaux, S., & Tielens, A. G. G. M. 2004, ApJ, 604, 222
Chang, Q., Zheng, X.-L., Zhang, X., et al. 2021, RAA, 21, 039
Chevance, M., Krumholz, M. R., McLeod, A. F., et al. 2022, arXiv:2203.09570
Cuppen, H., & Herbst, E. 2007, ApJ, 668, 294
Das, A., Sil, M., Ghosh, R., et al. 2021, FrASS, 8, 671622
Garrod, R. T., Wakelam, V., & Herbst, E. 2007, A&A, 467, 1103
Gould, R. J., & Salpeter, E. E. 1963, ApJ, 138, 393
Grassi, T., Bovino, S., Caselli, P., et al. 2020, A&A, 643, A155
Gry, C., Boulanger, F., Nehmé, C., et al. 2002, A&A, 391, 675
Herbst, E., & Klemperer, W. 1973, ApJ, 185, 505
Hincelin, U., Chang, Q., & Herbst, E. 2015, A&A, 574, A24
Iqbal, W., Acharyya, K., & Herbst, E. 2012, ApJ, 751, 58
Iqbal, W., Acharyya, K., & Herbst, E. 2014, ApJ, 784, 139
Meng, Q., Chang, Q., Zhao, G., et al. 2023, MNRAS, 526, 2394
Nakazato, Y., Chiaki, G., Yoshida, N., et al. 2022, ApJL, 927, L12
Pierre, L., Guignes, H., & Lhuillier, C. 1985, JChPh, 82, 496
Sternberg, A. 2006, The Physics and Chemistry of Interstellar Molecular Clouds: Proc. 2nd Cologne-Zermatt Symposium (Berlin: Springer), 175
Tacconi, L. J., Genzel, R., & Sternberg, A. 2020, ARA&A, 58, 157
Tielens, A. G., & Allamandola, L. J. 1987, Interstellar Processes: Proc. Symp. on Interstellar Processes (Berlin: Springer), 397
Tiné, S., Lepp, S., Gredel, R., & Dalgarno, A. 1997, ApJ, 481, 282
Tsuge, M., Hama, T., Kimura, Y., Kouchi, A., & Watanabe, N. 2019, ApJ, 878, 23
Vidali, G., Ihm, G., Kim, H.-Y., & Cole, M. W. 1991, SurSR, 12, 135
Wakelam, V., Bron, E., Cazaux, S., et al. 2017, MolAs, 9, 1
Watson, W., & Salpeter, E. 1972, ApJ, 174, 321
Zhao, G., Chang, Q., Zhang, X., et al. 2022, MNRAS, 512, 3137